Cyclic Nonlinear Behavior of a Glassy Polymer Using a Contact Method

Eric Janiaud,[1,2] Antoine Chateauminois,[1] Christian Fretigny[1]

[1]Laboratoire de Physico-Chimie des Polymères et des Milieux Dispersés (PPMD), UMR CNRS 7615, Ecole Supérieure de Physique et de Chimie Industrielles (ESPCI), Université Pierre et Marie Curie (UPMC), 10 rue Vauquelin, 75231 Paris Cedex 5, France

[2]Dutch Polymer Institute (DPI), Technishe Universiteit Eindhoven, PO BOX 902, 5600 AX Eindhoven, The Netherlands

Correspondence to: A. Chateauminois (E-mail: antoine.chateauminois@espci.fr)

ABSTRACT: The effects of repeated large strain shear cycles on the dynamics of a glassy acrylate polymer are investigated using an original contact method. It is based on the measurement of the shear properties of thin (about $50\,\mu m$) polymer films geometrically confined within contacts between elastic substrates. Under small amplitude ($300\,nm$–$10\,\mu m$) oscillating lateral displacements, friction at the contact interface can be neglected and the measurement of the contact lateral response thus provides information about the rheology of the sheared polymer film. Using this approach, the complex shear modulus of the polymer film can be measured both in the linear (viscoelastic) and in the nonlinear regimes. The investigations are focused on the changes in mechanical properties induced in a large strain regime where the polymer glass is cyclically sheared up to the yield point. During the application of large strain cycles, the mechanical response of the polymer glass slowly evolves toward a quasi stabilized state which is described from the measurement of an apparent–strain dependent–complex shear modulus. When the applied strain is increased by a tenfold factor, this apparent shear modulus decreases by about one decade. These underlying changes are investigated from a consideration of the time dependent linear viscoelastic properties after the mechanical stimulus. Both mechanical rejuvenation and recovery (ageing) effects are evidenced. © 2011 Wiley Periodicals, Inc. J Polym Sci Part B: Polym Phys 49: 599–610, 2011

KEYWORDS: amorphous; contact; film; glassy polymer; mechanical properties; mechanical rejuvenation; physical ageing; plasticity; shear; thin films; yielding

INTRODUCTION Polymer glasses are out of equilibrium systems characterized by a very broad spectrum of relaxation times. The segmental mobility characterized by this spectrum results in the spontaneous occurrence of slow structural relaxation processes referred to as physical ageing. This concept was first introduced by the seminal work of Struik[1] who also suggested that mechanical stimulus can disturb physical ageing processes, mainly by creating additional free volume in the perturbed glassy polymer. Specifically, early experimental studies led Struik to conclude that the application of a high stress reactivated physical ageing processes. From an analogy with the thermal rejuvenation process which occurs after quenching a polymer glass from above T_g, the effect of large mechanical stresses on the dynamics of the polymer glass was termed mechanical rejuvenation by Struik. Reactivated ageing processes induced by the mechanical stimulations of polymer glasses were later evidenced experimentally by Aboulfaraj et al.[2] from an investigation of the build up of yield stress following large strain cycling in the plastic regime. From an energy landscape perspective, it was later argued by Lacks and Osborne[3] that rejuvenation is caused by the strain induced disappearance of energy minima when plastic deformation occurs: a cycle of large strain thus rejuvenates the glass by reallocating the system to shallower energy minima. In that sense, the occurence of a mechanical rejuvenation process implies that the mechanical stimulus not only results in a departure from the local equilibrium but that it also alters the underlying structure of the glass. These issues are essential in the modeling of the nonlinear behavior of polymers which, according to O'Connell and McKenna,[4] cannot be simply handled through simple time-temperature and time strain superposition principles following early suggestions by Bernstein.[5]

The relevance of the mechanical rejuvenation concept was largely debated[6–8] with the conclusion that the deformation of polymer glasses results in a new thermodynamic state which is largely different from that achieved after thermal rejuvenation. The microstructural rearrangements that occur during large strain compression of glassy polymers were analyzed by Hasan and Boyce[9] from differential scanning calorimetry (DSC) measurements. These authors came to the conclusion that the rearrangements associated with inelastic deformation act to store energy locally, thus biasing and reducing the

activation energy barrier for structual rearrangements. Some insights into the nature of these rearrangements were recently provided by Casas et al.[10] from elastic neutron scattering of cold drawn acrylates. These authors showed that the plastic deformation is homogeneous and is affine at scales larger than about half the entanglement distance. However, at length scales about the monomer size, the structure of the stretched polymer chains remains nearly isotropic but appears also slightly distorted by the plastic deformation. From Molecular Dynamics simulations, Hoy and Robbins[11,12] also reviewed critically the role of entropic contributions during the strain hardening of glassy polymer with an emphasis on the effects of entanglement and chain orientation.[11,12] Direct atomistic simulations of PC glass by Lyulin and Michels[13] also showed that the partitioning of the internal energy is completely different for thermally and mechanically rejuvenated polymers. From macroscopic mechanical experiments, much evidence was accumulated to associate the structural change—or rejuvenation—of polymer glasses with the strain softening process observed at the yield point (see e.g., Boyce and Arruda,[14] G'Sell and Souahi,[15] Meijer et al.[16] and Buckley et al.[17]). Positron annihilation lifetime spectroscopy experiments carried out after mechanical deformation led Hasan et al.[18] to conclude that an increase in free volume with inelastic straining accompanies this strain softening mechanisms. Mechanical experiments at large strain also support the idea that yielded polymers exhibit an enhanced segmental mobility as a result of structural rearrangements.[19–22] Recently, Lee et al.[23–25] probed directly the segmental dynamics of a polymer glass (PMMA) using an optical photobleaching technique. They showed that segmental mobility can indeed increase by orders of magnitudes upon the application of tensile creep.

In most of these experimental studies, the dynamics of the polymer glass is probed during or after the application of a monotonic or static plastic deformation. In such a loading procedure, the mechanical stimulus mixes many time scales. Moreover, it also results in a continuously evolving structural state of the glass which complicates the physical analysis of the glass dynamics. On the other hand, early experimental work by Rabinowitcz and Beardmore[26] indicates that amorphous polymers submitted to repeated cyclic deformations in the nonlinear regime slowly evolve toward a steady state, while the time scale of the mechanical stimulus is controlled through its frequency. However, attempts to investigate the changes in the structure and dynamics of polymers in the large strain cyclic regime using conventional tensile or shear mechanical experiments are invariably complicated by the occurrence of defects such as crazes or fracture.[26–28]

In this article, we introduce an alternate approach based on a contact method where a thin polymer film is cyclically sheared within a contact between elastic substrates. This method presents the advantage of preventing crack formation during the application of large amplitude cyclic deformations by virtue of the contact pressure. In addition, the use of moderately thin films (about 50 μm) avoids self-heating processes which occurs invariably during large strain cyclic loading of bulk specimens.[29] We take advantage of this method to

prepare a polymer glass in a quasi steady-state by the repeated application of shear cycles in the nonlinear regime. This preparation step is carried out at increasing strain amplitudes up to the yield strain of the polymer. The dynamics of the mechanically stimulated system is subsequently analyzed in the light of small strain linear viscoelastic measurements carried out at imposed frequency. In the first part of this article, we describe the contact method and the associated methodology. In Experimental section, we focus on the analysis of the time dependent viscoelastic properties of the glass during and after the application of large strain cycles. Mechanical rejuvenation and recovery processes are evidenced for which the characteristic time scales are analyzed as a function of the strain amplitude and frequency of the large strain preparation.

EXPERIMENTAL

Materials

A crosslinked acrylate polymer was selected as a glassy system.[30] It was obtained from the copolymerization of n-butylmethacrylate (Acros Organics, purity 99%) and isobutylmethacrylate (Acros Organics, purity 99%) in a 1.2:1.0 molar ratio. The crosslinking agent was butanedioldiacrylate (Lancaster, 85%) with a concentration of 4 mol L^{-1}. Irgacure 819 (Ciba Specialty Chemicals) was used as an initiator for the UV polymerization of the mixture. The films were formed by casting the prepolymerized monomer mixture between two glass plates separated by a spacer. One of the glass plates was functionalized with a coupling agent (3-methacryloxy-propyl-dimethylchlorosilane) to promote chemical bonding with the acrylate layer. The other glass plate was treated with a release agent (dimethylchlorosilane). After UV curing, an additional heat treatment at 120 °C under vacuum was carried out for 12 h to increase the extent of reaction and to eliminate residual unreacted monomers. Film thickness was systematically measured using an optical profilometer at different locations within each specimen. Depending on the film specimen, the average thickness was found to vary between 53 and 58 μm. The glass transition of the acrylate polymer is $T_g = 53$ °C, as measured by DSC at 10 °C min^{-1}.

Dynamic mechanical thermal analysis (DMTA) measurements have been carried out using the same acrylate system in bulk form. The complex Young's modulus was measured at frequencies ranging from 0.1 to 25 Hz during isothermal steps. The temperature of the isothermal steps was increased by 2 °C increments from 15 to 120 °C. At each temperature step, data were acquired after a 2 mn thermal equilibration time. From these experiments, a master curve giving the storage and loss components of the Young's modulus was obtained at a reference temperature, $T_{ref} = 23$ °C (cf. Fig. 1). In addition, the yield properties of the bulk acrylate were measured in compression using cylindrical specimens. The yield strain and stress were found to be 6.4% and 37 MPa, respectively, at 25 °C and at a strain rate equal to 10^{-2} s^{-1}.

Lateral Contact Experiments

Cyclic shear experiments were carried out using a lateral contact method where the polymer film bonded to the glass flat is
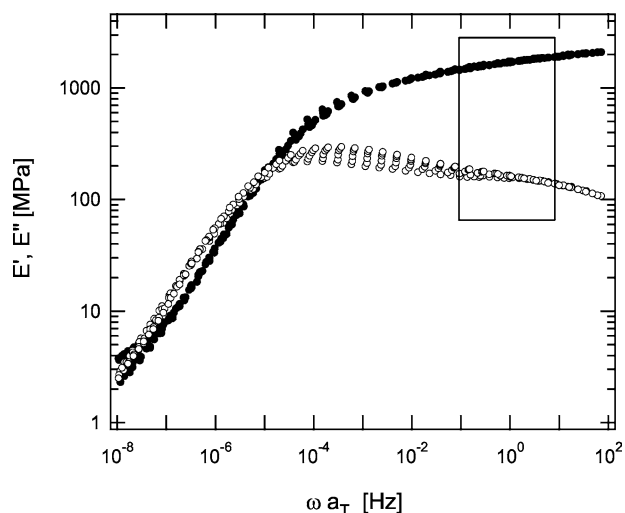
FIGURE 1 Master curve giving (•) the storage, E' and (○) loss, E'' components of the complex Young's modulus of the crosslinked acrylate as a function of the reduced frequency at 23 °C. D.M.T.A. measurements carried out using a bulk specimen. The box delimits the available frequency range during contact experiments.

sheared within a contact (a few hundreds of μm in diameter) with a spherical glass lens (Fig. 2). Provided that the displacement is kept low enough (i.e., in the nm–μm range), the film can be sheared without significant microslip at the contact interface. In such a situation, the contact lateral response provides information about the rheology of the polymer film sheared within the contact interface. The principle of such an experiment has already been described and validated in the small deformation regime using a home made contact device.[30,31]

For the purpose of the present study, a new, more accurate and versatile, version of this contact device has been developed. The apparatus is based on a combination of leaf springs loaded in tensile (along the normal direction) and bending (lateral direction) modes to ensure a high (resp. low) stiffness in the normal (resp. lateral) direction (normal stiffness >1 N/μm; lateral stiffness <0.02 N/μm), while ensuring an efficient mechanical decoupling of the loading applied along these two directions. By means of a piezoelectric actuator, a small amplitude sinusoidal lateral displacements is imposed to the glass lens while the coated glass substrate is fixed within a stiff specimen holder. The piezoelectric actuator is operated in closed loop control with an optical displacement transducer which monitors continuously the lateral motion of the lens. The lateral force is measured using a piezoelectric sensor in series with the actuator. Pictures of the contact region taken through the glass lens are also recorded by means of a microscope objective, a CCD camera and a frame grabber. During each shear cycle, the lateral force and displacement are continuously recorded to get the complex lateral contact stiffness defined as $K^* = F^*/\delta$, where F^* is the complex lateral force and δ is the displacement amplitude at the considered frequency. A complex shear modulus is deduced from this measured lateral

stiffness using an approximate coated contact model which was already validated in the small strain regime with the used acrylate system.[31] As it is recalled in the appendix, this contact model assumes a linear viscoelastic response of the polymer film within the shear loaded zone. When large strains are applied to the film, it only provides an apparent—nonlinear—shear modulus which must not be assimilated to the linear viscoelastic modulus measured under a small strain condition. Another assumption of the model is that the mechanical properties of the film are uniformly distributed within the contact zone. Such an hypothesis is questionable after the application of large strain cycles due to heterogeneous contact deformation. As strain induced changes in the mechanical properties of polymers are known to be controlled by the local deformation, the polymer film could display a variation of its viscoelastic properties throughout the shear loaded zone after the occurrence of large strain cycles. However, such heterogenities can be assumed to be limited due to the geometrical confinement of the film between the elastic glass substrates. Nonuniform deformation of the confined film is likely to occur mostly at the periphery of the contact, over a length of the order of film thickness (i.e., about 50 μm). The ratio of the contact radius to the film thickness being greater than 7 in all our experiments, the contribution of the strain inhomogeneities to the lateral contact response should therefore be limited.

A borosilicate glass lens (Melles Griot, France) with a radius of curvature of 14.8 mm is used in all the experiments. Before use, it is carefully cleaned in acetone, rinsed with ethanol and dried under nitrogen. Further treatment of the glass lens by air plasma for 5 min is carried out to promote a good adhesion with the acrylate film which in turn increases the displacement threshold for the occurrence of microslip. A normal load in the range 5–50 N is applied to the lens to form a contact. The resulting initial mean contact pressure is about 90 MPa. From a previous investigation of the
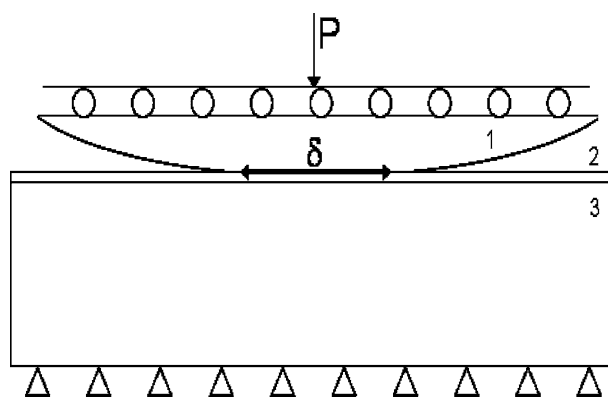
FIGURE 2 Schematic description of the contact configuration. A glass lens (1) is contacting a flat glass (3) substrate coated with the polymer film (2) under a constant normal applied force, P. To shear the polymer film, a small amplitude sinusoidal lateral motion is applied to the lens along the horizontal axis. Care has been taken to align the lateral loading axis with respect to the contact point to avoid the application of a torque to the lens.

indentation behavior of the acrylate film under consideration,[32] this contact pressure was found to correspond to the boundary between the elastic and plastic indentation behavior for the considered film thickness and lens radius. It can be noted that this mean contact pressure at the onset of yield is much larger than the compression yield stress measured using bulk cylindrical specimens of the same acrylate (i.e., 37 MPa at 10^{-2} s^{-1} and 25 °C). Such a difference obviously arises from the differing loading geometry but it could also incorporate some hydrostatic pressure effects. As detailed in reference,[32] variations in the indentation yield stress of the studied acrylate film when the contact conditions are changed can be accounted for by the well known sensitivity of the yield properties of polymer to hydrostatic pressure.[33]

During lateral contact experiments, a sinusoidal displacement with an amplitude ranging from 0.3 to 6 μm is applied to the contact. The corresponding nominal shear strain amplitude, $\gamma_0 = \delta_0/t$, where δ_0 is the displacement amplitude and t is the film thickness, varies from 0.6 to 10%. Available frequencies lie in the range 0.01–8 Hz. All the experiments reported here are performed at room temperature (20–25 °C). By virtue of the thin film geometry, only a limited polymer volume is sheared which can easily exchange heat with the surrounding glass substrates. As a result, only a very limited heating (less than 0.5 °C) of the film occurs within the investigated strain and frequency range. This was demonstrated from thermal calculations and confirmed experimentally from preliminary infrared thermal contact imaging experiments. As opposed to many large strain cyclic mechanical experiments using bulk polymers where self heating of the specimen is a concern,[29] the present contact experiments are thus carried out under isothermal conditions. As a check of the reproducibility of the experiments, the linear viscoelastic modulus of the virgin polymer film was measured at 1 Hz and at room temperature for 30 different contacts on different film specimens. In this reference state, the storage and loss components of the shear modulus were found to be $G' = 1055 \pm 45$ MPa and $G'' = 64 \pm 4$ MPa, respectively (i.e., $\tan \delta = 0.061 \pm 0.003$).

RESULTS AND DISCUSSION

Contact Response During and After the Application of Large Strain Cycles
We detail here an experiment consisting of the following two successive steps: (i) a sequence of 1000 large strain amplitude cycles within the nonlinear regime ($\gamma_0 = 6.0\%$, 1 Hz) followed by (ii) a step where the changes in the linear viscoelastic modulus of the mechanically stimulated film are continuously monitored at a low strain ($\gamma_0 = 0.7\%$, 1 Hz) during 1000 s.

Large Strain Contact Response
Contact Creep
During the application of large strain shear cycles under a constant applied normal load, a contact creep process is observed. As shown in Figure 3, the contact radius slowly increases up to about 15% of its initial value after 1000 cycles. Profilometry measurements carried out in the contact zone (see inset in Fig. 3) show that a permanent spherical imprint is left in the
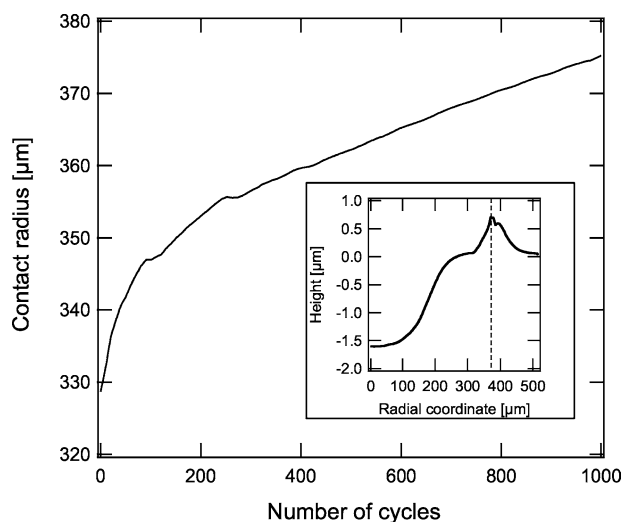
FIGURE 3 Contact radius as a function of the number of cycles in the large strain regime ($\gamma_0 = 6\%$, 1 Hz). Inset: radial profile of the imprint left at the surface of the film after 1000 cycles (the dotted line delimits the contact radius).

polymer film at the end of the mechanical cycling step. It was verified from profilometry measurements that complete healing of the imprint takes place when the film is annealed above T_g. This observation tends to indicate that no permanent contact damage is involved in the formation of the contact imprint. It was also noted that, under the action of a purely normal contact load, a much more limited contact creep is observed. The formation of the imprint thus results from the combined action of the normal and lateral loads. These phenomena are reminiscent of the so-called "junction growth" mechanism proposed by Bowden and Tabor[34] for frictional contacts in the plastic regime. Basically, the argument is that, when a single asperity contact is sheared under a constant normal load in the plastic regime, the observation of the yield criterion implies that the contact should grow during the application of the lateral force.

According to the contact model recalled in appendix, one of the consequences of the contact creep process is an enhancement of the contact stiffness for given film and substrate shear properties. To account for this effect in data analysis, a time dependent radius $a(t)$ is introduced in eqs 2 and 3 which express the relationship between the complex modulus and the complex contact stiffness. Another effect of contact creep is to induce a slight permanent decrease in film thickness which questions the validity of modulus measurements using the initial film thickness as a reference. However, one may argue that the maximum depth of the imprint (about 1.5 μm) represents less than 3% of the film thickness and that this effect is probably negligible. Additionally, it was verified that such a limited reduction in thickness has a minor effect on the determination of the complex shear modulus using eqs 2 and 3. More importantly, the contact creep process under a constant applied normal load results in a progressive decrease in the mean contact pressure. As discussed in the next section, this evolving contact pressure affects the modulus measurements
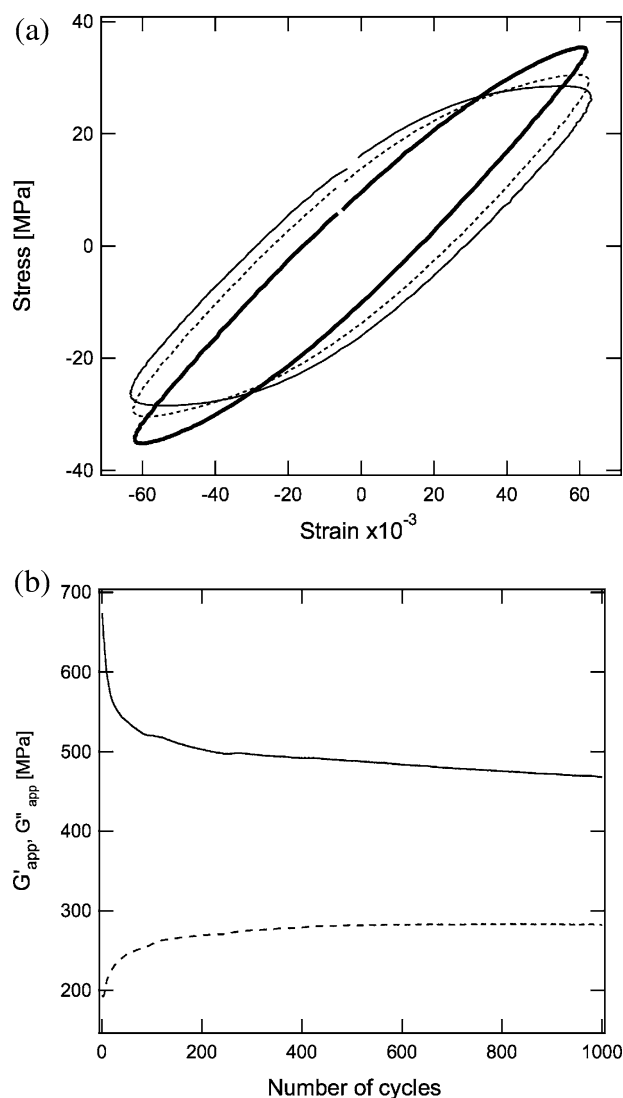
FIGURE 4 Nominal stress-strain behavior in the large strain regime ($\gamma_0 = 6\%$, 1 Hz). (a) Lissajou representation of the stress-strain relationship at different number of cycles. Bold line: 2^d cycle, dotted line: 60th cycle, continuous line: 100th cycle. (b) Apparent nonlinear shear moduli G'_{app} (plain line) and G''_{app} (dotted line) as a function of the number of cycles.

as a result of the sensitivity of the mechanical properties of polymer glasses to hydrostatic pressure.

Stress/Strain Behavior and Apparent Shear Modulus

From the measured lateral force, F, and displacement, δ, one may define nominal stress and strain as $F/\pi a^2$ and δ/t, respectively, where a is the measured contact radius and t is the film thickness. When reported in a Lissajou representation [Fig. 4(a)], this stress/strain relationship rapidly evolves from a nearly elliptic cycle toward a slowly evolving response which is characterized by a decreased maximum stress and enhanced dissipative processes (as indicated by increasing cycle opening). A strain and time dependent apparent shear modulus,

G^*_{app}, can be ascribed to this nonlinear response which is determined from the in-phase and out-of-phase components of the lateral contact stiffness at the considered excitation frequency. In Figure 4(b), the storage (G'_{app}) and dissipative (G''_{app}) components of this apparent shear modulus are reported as a function of the number of shear cycles. A strong drop in G'_{app} and a corresponding increase in G''_{app} are evidenced which reflect strong changes in the glass dynamics. Most of these changes occur within about 50–100 cycles. Then, a slow drift of G'_{app} and G''_{app} takes place at longer times.

This long term drift may be attributed to a pressure dependence of the apparent shear modulus: by virtue of contact creep, the mean contact pressure during the application of cyclic nonlinear strain is continuously decreasing from its initial value (90 MPa) to about 65 MPa. Mechanical properties of polymers being sensitive to hydrostatic pressure,[35] one could therefore tentatively attribute the long term changes in G^*_{app} to the decreasing contact pressure. Within the linear viscoelastic regime, strong effects of the contact pressure on the shear modulus were already reported by Chateauminois et al.[32] in the glass transition zone using the same thin film contact geometry. To estimate the pressure sensitivity of the apparent shear modulus, measurements of G'_{app} were carried out as a function of contact pressure under conditions where kinetics effects are no longer involved. For that purpose, a contact is first prepared in the nonlinear regime by applying 240 shear cycles at a strain of 8%. Then, G'_{app} is measured during short (60 cycles) sequences carried out at various contact pressure (between 45 and 70 MPa) and at two different strain amplitudes (5 and 8%). During each of these measurements, the contact radius remained constant within 1%, thus ensuring that creep was negligible. Results in Figure 5 reveals that G'_{app} is a linearly increasing function of the mean contact pressure, p_m. The slope, $\partial G'_{app}/\partial p_m$, is equal to 3.6 and 2.4 for $\gamma_0 = 5\%$ and $\gamma_0 = 8\%$, respectively. These values are of the same order of magnitude than those reported in the literature for the linear shear modulus of poly(methylmethacrylate).[36–38] On the other hand, a much lower sensitivity of the yield stress to hydrostatic pressure was reported Rabinowitz et al.[33] for acrylate polymers such as poly(methylmethacrylate) ($\partial \sigma_y/\partial p_m = 0.25$). The observed pressure dependence of the apparent shear modulus can therefore not be accounted for solely from a consideration of the increase in the yield stress of the material with the contact pressure.

It is also noteworthy that, while our contact device was unable to detect any very significant pressure induced change in the linear storage modulus G' at room temperature within the range 40–100 MPa, a measurable pressure dependence is observed in the large strain regime. If one recalls that the pressure dependence of the modulus of glassy polymers is drastically enhanced in the glass transition zone,[32,35] this difference in the presssure dependency of the shear behavior between the linear and nonlinear regimes could thus be interpreted as evidence of a depressed glass transition temperature in the loaded and deformed state. This hypothesis is further supported by the linear viscoelastic measurements reported in the next section.
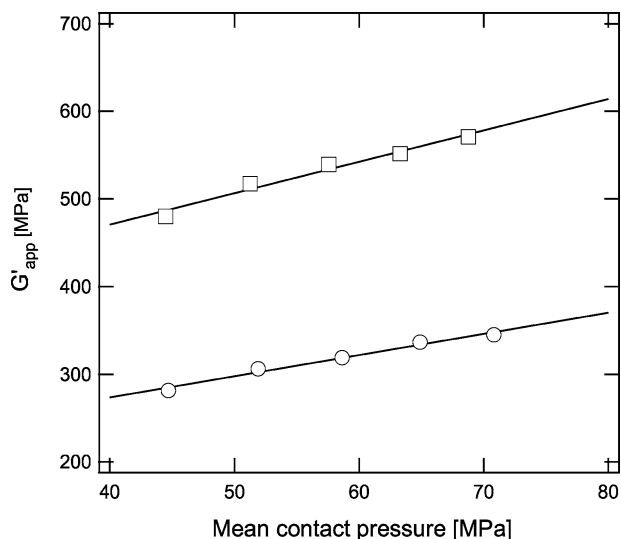
FIGURE 5 Pressure dependence of the storage component of the apparent shear modulus, G'_{app}, in the large strain regime (1 Hz). ($\square$) $\gamma_0 = 5\%$; ($\circ$) $\gamma_0 = 8\%$. Data were obtained after a contact preparation consisting in the application of 240 cycles at $\gamma_0 = 8\%$ and 1 Hz (see text for details).

Strain Dependence of the Shear Modulus

The boundary between the linear viscoelastic and the nonlinear regimes was determined from an examination of the dependence of the shear modulus on strain amplitude (Fig. 6). For applied strain levels less than about 1%, a time and strain independant shear modulus is measured which corresponds to the expected linear viscoelastic response at the considered frequency. Above this strain threshold, the occurrence of a nonlinear response is indicated by a decrease in modulus with increasing strain amplitude. The apparent modulus values reported in Figure 6 correspond to the quasi stabilized state (i.e., for $N > 100$ cycles). As creep occured to various extents depending on the magnitude of the applied strain, the associated contact pressures were thus different. To account for the contact pressure dependence of G'_{app}, the values corresponding to the various strain levels were linearly interpolated to a pressure equal to 75 MPa assuming a linear dependence of the modulus on the contact pressure (cf. Fig. 5). In passing, it can be noted that the observed linear behavior is reminiscent of the so-called Payne effect reported in filled elastomers (see ref. 39 for a review). Under medium to large cyclic strains, filled elastomers exhibit a markedly nonlinear response which is absent in unfilled systems. An order of magnitude drop in the modulus is commonly observed on going to 5–10% deformation under shear which is similar to the measured decrease for the glassy acrylate film under consideration. Such a similarity between the nonlinear behavior of filled rubbers and glassy polymers could tentatively be accounted for within the framework of a description proposed by Lequeux and coworkers.[40,41] These authors have shown than filler particles within the rubber matrix can be embedded within a glassy shell due to the restricted mobility of the polymer chains at the particle surfaces. According to the present results, strain softening in filled rubbers could thus arise from the cyclic plastic deformation of glassy bridges between neighboring particles.
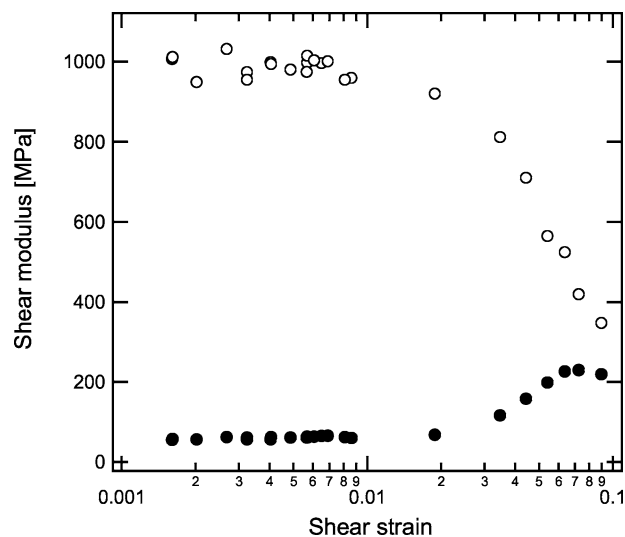
FIGURE 6 Storage ($\circ$) and loss ($\bullet$) components of the complex shear modulus as a function of the applied nominal strain (1 Hz). For strain levels less than about 1%, data correspond to the linear viscoelastic shear moduli (G' and G''). Above this strain threshold, an apparent nonlinear shear modulus (G'_{app} and G''_{app}) is measured. Data in the nonlinear regime were interpolated to a contact pressure of 75 MPa (see text for details).

Time Dependent Changes in the Linear Viscoelastic Properties After Large Strain Cycles

Immediately at the end of the large strain step, a small amplitude ($\gamma_0 = 0.7\%$) cyclic shear at 1 Hz is applied to the contact to probe the linear viscoelastic response of the mechanically stimulated polymer glass. A decrease in G' and a corresponding increase in G'' are first observed (Fig. 7). As compared to the initial (i.e., before large strain cycles) viscoelastic modulus ($G' = 1100$ MPa, $G'' = 67$ MPa), the storage modulus at 1 Hz is
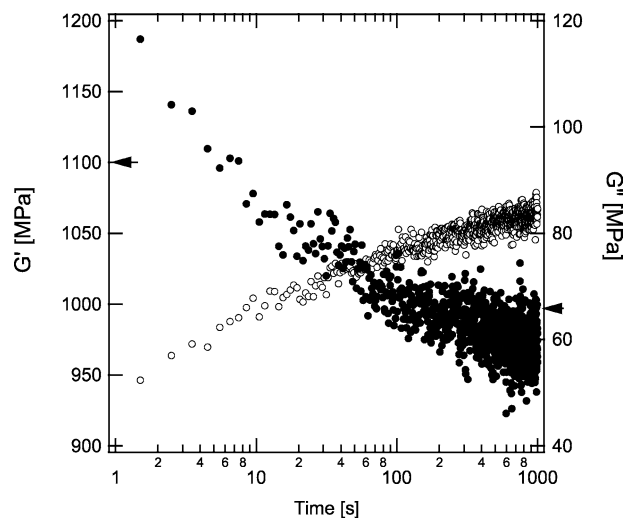
FIGURE 7 Time dependent changes in the linear viscoelastic shear modulus ($\gamma_0 = 0.7\%$ 1 Hz) after the application of 1000 strain cycles in the large strain regime ($\gamma_0 = 6\%$, $F = 1$ Hz). ($\circ$) G', ($\bullet$) G''. Arrows on the left and right axis indicate the values of G' and G'' before the application of large strain cycles.
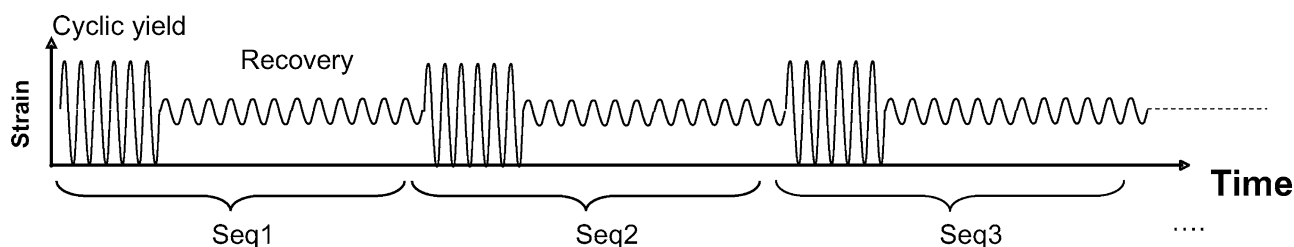
FIGURE 8 Schematic of the sequential loading history applied to the acrylate films: large strain amplitude sequences are alternated with small strain amplitude sequences where the linear viscoelastic modulus is continuously monitored as a function of elapsed time.

decreased by about 15% and the loss modulus is increased by about 75%. Such a change in the viscoelastic modulus can be described as a mechanical rejuvenation effect in the sense that it reflects an enhanced mobility within the cyclically deformed polymer glass. Moreover, the linear viscoelastic moduli slowly recovers toward its initial value on an essentially logarithm time scale (Fig. 7).

This recovery may be viewed as evidence of an enhanced physical aging rate within the mechanically stimulated glass (as afore mentioned, no time dependent change in the linear viscoelastic properties of the virgin polymer was detected within the experimental time frame). However, full recovery of the linear viscoelastic modulus to its initial value is not observed within the considered ageing time. Figure 7 shows that G' remains below its initial value (1100 MPa) and that G'' is also slightly depressed below its reference value (67 MPa) after 1000 s ageing. When the film is heated above T_g (at about 70 °C) and cooled down again, its initial viscoelastic properties are fully recovered (results not shown) which demonstrates that no permanent damage is involved in the observed long term changes in G^* after the application of large strain cycles. In such a nonergodic system, one could state that full recovery would most likely not be posible. However, as mentioned by Bodiguel et al.,[42] the long term modulus of glassy polymers is only weakly sensitive to thermal or mechanical stimulus. Permanent changes in the shear modulus after large strain cyclic deformation should therefore be limited. At this stage, we are unfortunately unable to state whether the observed slight variations in G' and G'' after 1000 seconds are due to changes in the mechanical properties of the glass or to some uncertainty in the measurement of the radius of the deformed contact. As shown in Figure 3, some pile up occurs at the edge of the contact imprint which could result in an overestimate of the effective value of the contact radius. Calculations indicate that an error of 10 μm in the measurement of the actual contact radius could account for the permanent 50 MPa drop in G' after 1000 cycles.

Time and Strain Dependence of Mechanical Rejuvenation and Recovery Processes
Sequential Protocol

The time and strain dependence of mechanical rejuvenation and recovery processes was further examined using a sequential loading history where large and small strain cyclic steps are alternated within a given contact. As schematically depicted in Figure 8, we repeated five times within a given

contact a loading sequence consisting in the application of 60 cycles in the large strain regime (1 Hz) followed by a 240 s recovery step under a small strain condition. Figure 9 shows the changes in the storage and loss components of the apparent shear modulus during the successive large strain steps. After the application of the first block of 60 large strain cycles, it comes out that an invariant response is achieved during each of the subsequent large strain sequences. It is characterized by a rapid drop (resp. increase) in G'_{app} (resp. G''_{app}) followed by a slow drift along an envelope curve. As detailed before, this slow drift can be attributed to the pressure dependence of the apparent modulus, while the rapid drop mostly reflects the effects of the mechanical stimulus on the glass dynamics. The recovery of the linear viscoelastic modulus after each of the successive large strain periods was examined at 1 Hz. As shown in Figure 10, the recovery kinetics remains essentially invariant after all the large strain periods. As a consequence, G' and G'' data obtained during successive recovery steps can be averaged for a given set of large strain preparation conditions. Unless otherwise specified, all the recovery data reported below were obtained using this averaging procedure.
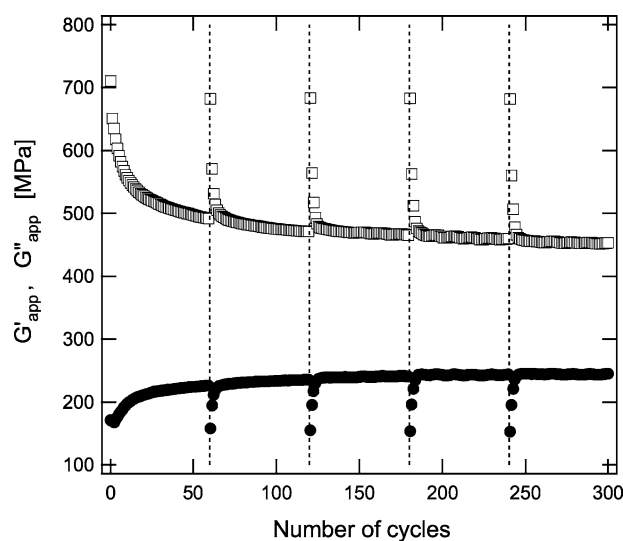
FIGURE 9 Storage G'_{app} ($\square$) and loss G''_{app} ($\bullet$) components of the apparent shear modulus as a function of the number of cycles in the large strain regime (sequential protocol, $\gamma_0 = 6.4\%$, $F = 1$ Hz). Sequences of 60 large strain cycles are alternated with 120 s recovery steps (not shown) which are indicated by dotted lines.
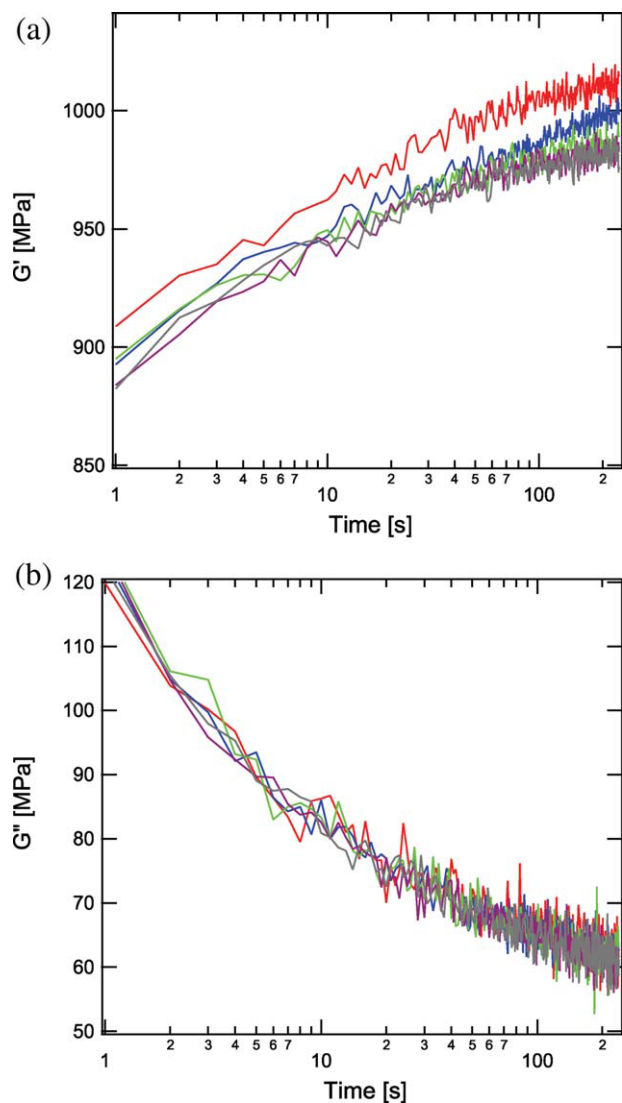
FIGURE 10 Recovery of storage modulus, G', and loss modulus, G'', at 1 Hz during successive small strain amplitude recovery sequences (sequential protocol). Before each recovery step, 60 cycles in the large strain regime ($F = 1$ Hz and $\gamma_0 = 6.4\%$) are applied to the film. Red, blue, green, purple, and gray lines correspond to increasing recovery sequence numbers.

Effects of Large Cyclic Strain on Recovery Processes

We now examine the dependence of recovery kinetics on the applied strain amplitude during the large strain preparation. For that purpose, the time dependent linear viscoelastic modulus is monitored for 240 s at 1 Hz after larges strain periods of 60 cycles (1 Hz) carried out at -30pc] strain amplitudes ranging from 2 to 9%. Figure 11, shows that the extent of the changes in G' and G'' are very sensitive to the applied strain during the large strain preparation. For $\gamma_0 = 2\%$, that is, just above the threshold of the nonlinear regime, almost no recovery is measured. On the other hand, when $\gamma_0 = 9\%$, G' decreases by 30% and G'' increases by 115% when compared to the reference state of the glass. An analysis of the relative changes in the linear viscoelastic properties reveals that the

amplitude of the applied strain in the nonlinear regime affects the magnitude of the recovery process rather than its kinetics. For that purpose, the relative changes in the loss factor $\tan \delta$ were considered because experimental results are less sensitive to small errors in the measurement of the contact radius of the contact. When reported in a log-log plot, the relative changes in $\tan \delta$ as a function of time after a large strain preparation at various strain levels fall onto straight lines with nearly identical slopes (Fig. 12). Recovery kinetics at short times (<200 s) thus follows an essentially power law dependence with time, that is, $\Delta \tan \delta = \beta t^\alpha$. While the prefactor β increases with applied strain, the exponent ($\alpha = -0.37 \pm 0.03$) is remarkably insensitive to this parameter. Alternatively, it
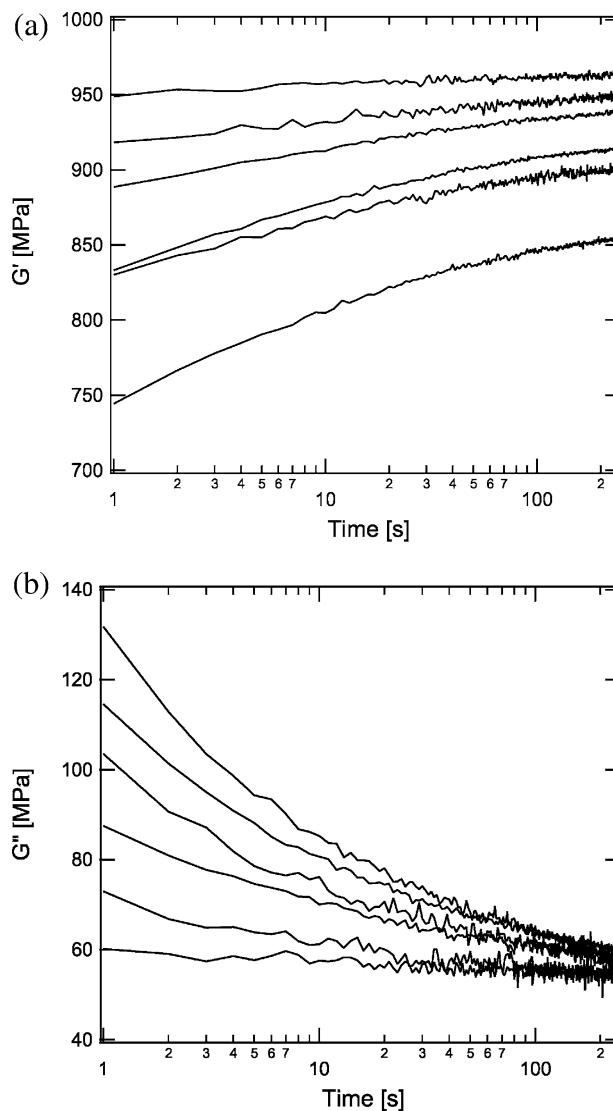
FIGURE 11 Recovery of the storage, G', and loss modulus, G'', ($\gamma_0 = 0.7\%$, $F = 1$ Hz) after the application of 60 large strain cycles at various strain levels (1 Hz). Data have been averaged over five successive recovery sequences. Applied strain amplitude: 1.9, 3.5, 4.4, 5.4, 6.4, and 9% from top to bottom (G' data) and bottom to top (G'' data).
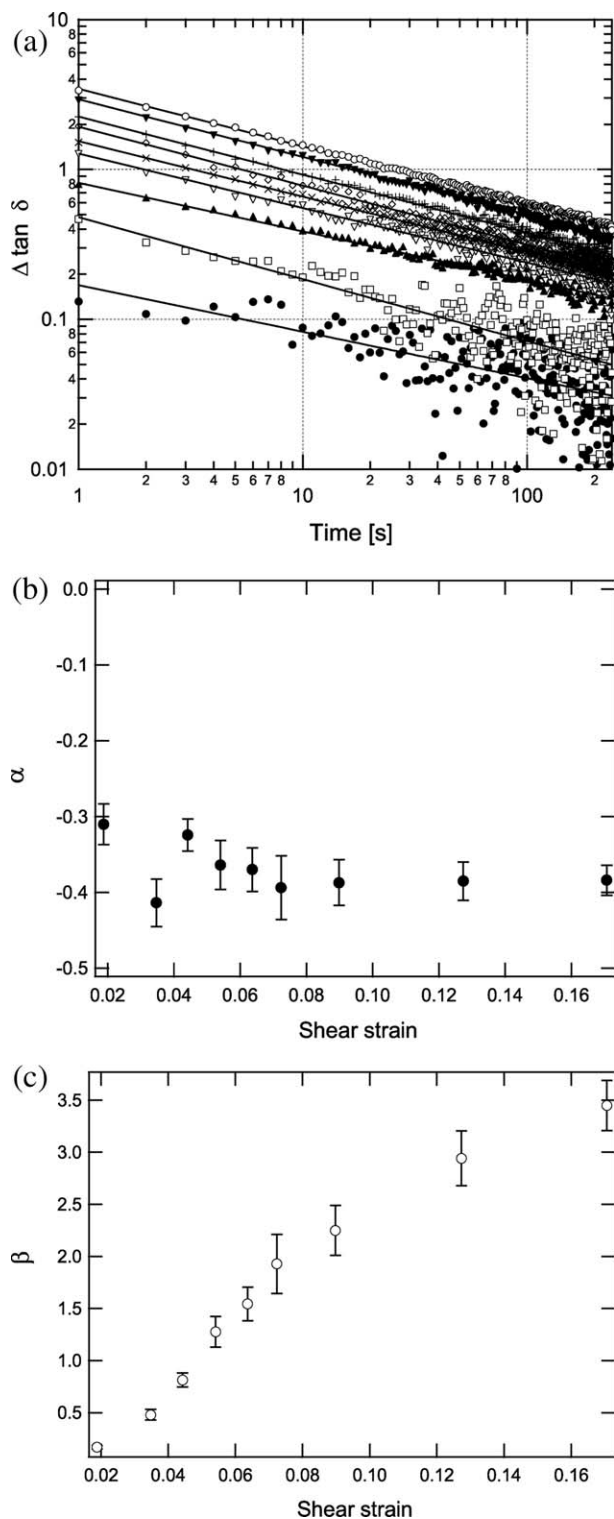
FIGURE 12 Relative changes in the loss factor, $\Delta \tan \delta = \frac{\tan \delta - \tan \delta_{ref}}{\tan \delta_{ref}}$, (1 Hz) as a function of time during recovery following large strain preparations at different strain amplitudes (1 Hz). $\tan \delta_{ref}$ is the loss factor measured before the mechanical stimulation. Applied strain amplitude: (•) 0.019, (□) 0.035, (▲) 0.044, (▽) 0.054, (×) 0.064, (◇) 0.072, (+) 0.090, (▼) 0.13, (○) 0.17. Solid lines correspond to power law fits, $\Delta \tan \delta = \beta t^{\alpha}$. The strain dependence of α and β is detailed in the bottom figures.

was attempted to fit the recovery data with a stretched exponential (results not shown). A characteristic time of the order of a few seconds was extracted from this fit which does neither change significantly with the applied strain. As a conclusion, it comes out that the recovery kinetics does not significantly depend on the strain applied in the nonlinear regime.

Frequency Dependence of Recovery

To probe the recovery at different frequencies, six different contacts are made on the same film but at different locations. The same large strain preparation consisting in 60 cycles at $\gamma_0 = 6.4\%$ and 1 Hz is applied to each contact before the recovery measurements which are carried out at frequencies ranging from 0.05 to 8 Hz. The number of cycles during the
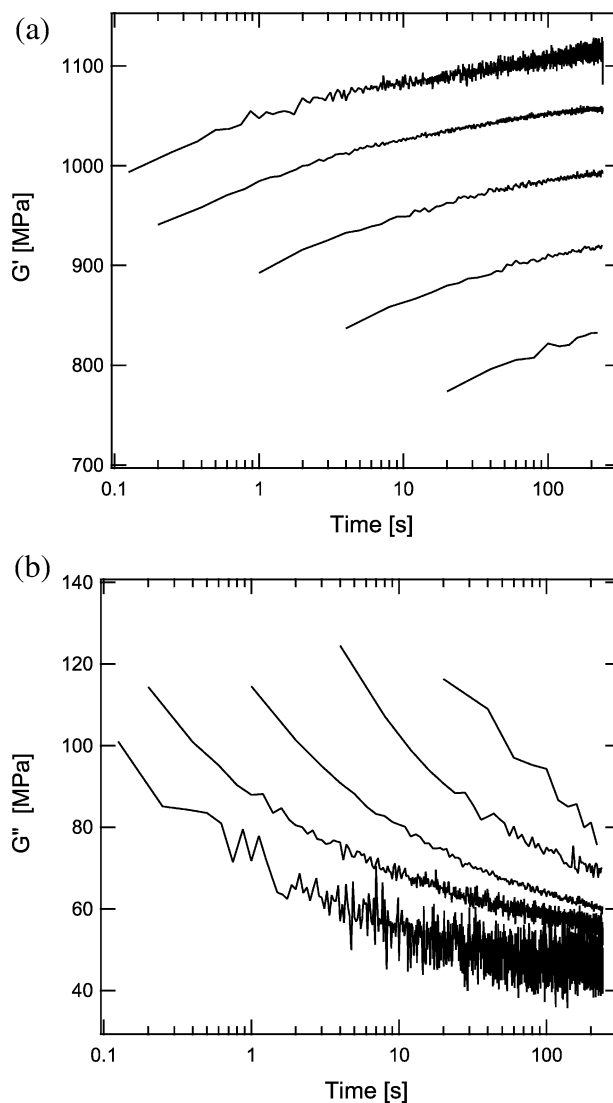
FIGURE 13 Recovery of the storage, G', and loss, G'', modulus at various frequencies. Increasing frequencies (0.05, 0.25, 1, 2.5, 5 and 8 Hz) from bottom to top (G' data) and from top to bottom (G'' data). The large strain preparation consisted in 60 cycles at $\gamma_0 = 6.4\%$ and $F = 1$ Hz. Data have been averaged over five successive recovery sequences.
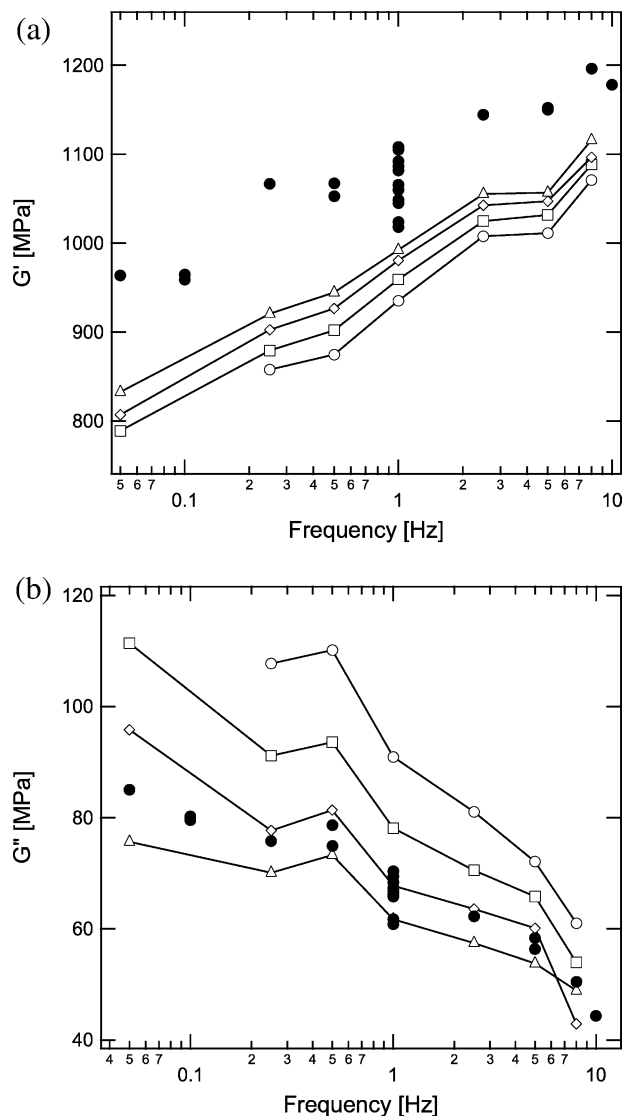
FIGURE 14 G' and G'' spectra at different times during recovery. (●) before the application of large strain, (○) 4 s, (□) 16 s, (◇) 64 s and (△) 240 s after cyclic preparation. The large strain cyclic preparation consisted in 60 cycles at $\gamma_0 = 6.4\%$ and 1 Hz (Same data as in Figure 13).

recovery step is ajusted to keep its duration constant (240 s). Time dependent changes in the linear viscoleastic modulus are reported in Figure 13. Alternatively, these data can be represented as a function of frequency for various recovery times (Fig. 14). When considering G'', there is some indication that the frequency dependence of the viscoelastic modulus is increased immediately after the application of large strain cycles. From these observations, one can speculate on the occurence of a shift of the G' and G'' spectra to high frequencies as a result of large strain mechanical stimulation. The observed changes in the shear linear viscoelastic modulus after the large strain cyclic preparation would thus be consistent with the hypothesis of a shift of the relaxation spectra to shorter times. This hypothesis is further supported by molecular

dynamics simulations of a poly(styrene) glass after a tension-compression cycle which show that large strain mechanical stimulation shifts the relaxation times distribution—both in α and β transition zones—to shorter times.[43] As a result of the increased segmental mobility within the mechanically stimulated glass, ageing is reinitiated as indicated by the progressive recovery of the viscoelastic properties.

When looking at the data in Figure 14, it also transpires that the spectra obtained at various recovery times could be shifted along the frequency axis to form a single master curve. Figure 15 shows the obtained master curve using tan δ and taking the virgin state as a reference. As shown in the insert in Figure 15, the horizontal shift factor log $a(t_r)$, where t_r is the recovery time, appears to be a linear function of the logarithm of t_r. It can be noted that the corresponding double logarithmic rate $\mu = \frac{d\log a}{d\log t} = 0.7$ is close to what is observed in thermal aging[1] where μ is often found to be close to unity. These observations present some analogy with an investigation by Aboulfaraj et al.[2] where the evolution of the yield stress was measured after a thermal quench or after the application of a shear strain cycle above yield. The build up of the yield stress after a thermal quench and after the large shear was found to follow a similar rate and also to have similar times to equilibration. However, the "equilibrium" values of the yield stress for the thermally quenched and for the mechanically stimulated material differ greatly, which was interpreted by Aboulfaraj et al. as evidence of a the occurrence of a "phase transition" within the yielded polymer. Data reported in Figure 11 also suggest that the equilibrium value of the shear modulus after the application large strain cycles might be lower than that of the thermally aged (i.e., in the so-called virgin state) polymer glass. However, one should be careful before drawing a
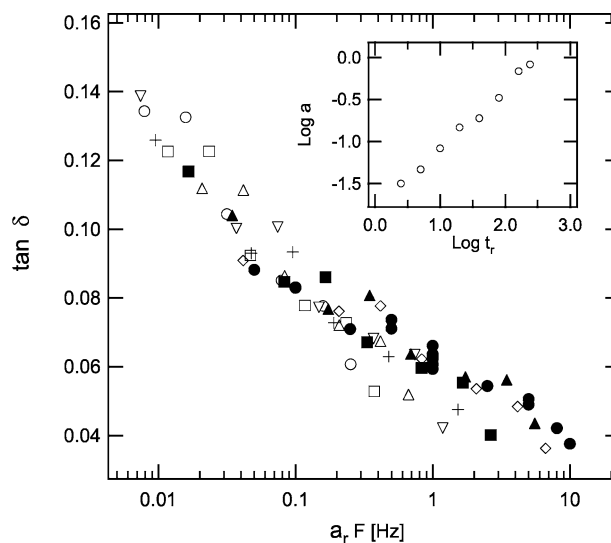
FIGURE 15 Master curve giving tan δ as a function of the frequency reduced by the ageing time. (○) 2.5 s, (□) 5 s, (△) 10 s, (▽) 20 s, (+) 40 s, (■) 80 s, (▲) 160 s, (◇) 240 s. Insert, shift factor log a versus log t_r. The large strain cyclic preparation consisted in 60 cycles at $\gamma_0 = 6.4\%$ and 1 Hz.

definite conclusion on that point due to uncertainties in the determination of the modulus after the occurence of contact creep, as detailed in Appendix.

CONCLUSIONS

The dynamics of glassy polymers in the cyclic nonlinear regime has been investigated using an original contact method where a thin film is sheared within a contact between elastic substrates. As compared to conventional mechanical testing using bulk specimens, this approach presents the advantage of preventing crack formation within the polymer during the repeated application of large strain cycles. In addition, it allows the investigation of the large strain cyclic behavior of polymer glasses under nearly isothermal conditions, that is, in the absence of self-heating phenomena. The investigations have been focused on the nonlinear shear properties of glassy acrylates systems up to the yield point. Under the action of large cyclic strains, the shear behavior of the polymer glass was found to evolve slowly toward a steady response. As opposed to monotonic loading, large strain cyclic deformation offers the possibility of preparing a deformed polymer glass in a stabilized state while the time scale of the mechanical stimulus remains controlled through its frequency. An apparent strain (and pressure dependent) shear modulus can be ascribed to this nonlinear response. The strain induced changes in the dynamics of the polymer glass were further investigated from linear viscoelastic measurements carried out after a preparation in the large strain regime. Both mechanical rejuvenation and recovery processes were evidenced from the measurement of the linear shear modulus: immediately after the application of large strain cycles, the storage modulus is depressed as compared to its initial value. Then, it slowly recovers on a nearly logarithmic time scale. These changes can be viewed as evidence of a shift of the relaxation time spectrum toward shorter times after the application of large strain cycles. Surprinsingly, the magnitude of the applied strain was found to affect the amplitude of the recovery process rather than its kinetics: the linear viscoelastic modulus recovers on a similar time scale after mechanical stimulation at applied strain amplitudes ranging from 2 to 10%. Although the reported mechanical rejuvenation effects could be anticipated from previous studies of polymer glasses in the plastic regime, the contact method emerges as a suitable approach to nonlinear cyclic loading. It could especially provide some insights into the memory effects involved in the ageing of glassy polymer systems.

ACKNOWLEDGMENTS

APPENDIX: RELATIONSHIP BETWEEN LATERAL CONTACT STIFFNESS AND COMPLEX SHEAR MODULUS

As detailed in reference,[31] a simple contact model can be derived within the limit of confined contact geometries (i.e., when the contact radius, a, is much larger than the film thickness, t, $a \gg t$) to relate the measured lateral contact stiffness, K^*, to the complex shear modulus of the film, G^*. We shall here only briefly recall the main ingredients of this approximate model. Within a mechanically confined contact, all the contact stresses applied to the film surface can be assumed to be integrally transferred to the film/substrate interface over a contact area of constant radius, a. Additionally, no sliding is assumed to take place at the interface between the lens and the polymer during lateral loading. In such conditions, the measured lateral contact stiffness can be modeled by considering two stiffnesses in series. The first stiffness component can be assimilated the pure shear response of the polymer disk enclosed with the contact. The second component corresponds to the elastic deformation of the substrates. Accordingly, one can express the lateral contact stiffness K as follows for a purely elastic system

$$\frac{1}{K} = \frac{1}{8 G_0^r a} + \frac{t}{\pi a^2 G} \tag{1}$$

where G is the film shear modulus and G_0^r is the reduced shear modulus of the substrates defined as $G_0^r = G_0/(2 - v)$ with G_0 and v the shear modulus and the Poisson's ratio of the substrate, respectively. In the above expression, the second term in the right handside corresponds to the shear response of the film. The first term describes the lateral stiffness of a bare sphere on flat elastic contact, as given by Mindlin's contact mechanics theory.[44] From the correspondence principle, this expression for a purely elastic contact can be generalized to viscoelastic systems, thus allowing to relate the complex shear modulus $G^* = G' + iG''$ with to the in-phase and out of phase components of the contact stiffness, $K^* = K' + iK''$. Then, inverting eq 1 provides the following expressions for G' and G''

$$G' = \frac{1}{D} \left(K' - \frac{K'^2 + K''^2}{8 G_0 a} \right) \frac{d}{\pi a^2} \tag{2}$$

$$G'' = \frac{K''}{D} \frac{t}{\pi a^2} \tag{3}$$

with D:

$$D = 1 - \frac{2K'}{8 G_0 a} + \frac{K'^2 + K''^2}{(8 G_0)^2 a^2} \tag{4}$$

At a low strain (i.e., within the linear viscoelastic regime), a steady state response is achieved and G^* can be easily determined from Fast Fourier Transform (FFT) of the load and displacement signals. On the other hand, a transient–time dependent–lateral contact response is achieved during and after the application of shear cycles in the large strain regime. As a consequence, FFT can no longer be used to determine the in-phase and out-of-phase components of the shear modulus. Instead, the contact stiffness is

determined from a fit of the lateral force and displacement signals to a combination of sinus and cosine functions. A linear time drift has been added to the load signal fitting expression to account for the "fading" memory effect associated with changes in the magnitude of the applied strain. Accordingly, the lateral force is fitted to the follwing expression $F = A_0 + A_1 t + A_2 \sin \omega t + A_3 \cos \omega t$, where ω is the imposed pulsation, A_0 is the offset value and A_1 is the linear drift factor. We have checked that $\frac{dA_0}{dt} \approx A_1$. Once the different A_i have been determined, the phase lag between displacement and force is easily determined and $K^* = K' + iK''$ can be computed. The complex apparent shear modulus G^*_{app} is then deduced from eqs 2 and 3.

A spectral analysis of the lateral load signal in the quasi steady-state nonlinear regime shows that it includes a minor contribution from odd harmonics. These odd harmonics can incorporate two different contributions coming from (i) the nonlinear response of the acrylate film and (ii) some residual microslip occurring at the outermost periphery of the contact. As it is not possible to differentiate between these two contributions, no further analysis of these odd harmonics was attempted.

REFERENCES AND NOTES

1 Struick, L. C. E. Physical Aging in Amorphous Polymers and Other Materials; Elsevier: Amsterdam, **1978**.

2 Aboulfaraj, M.; G'Sell, C.; Mangelinck, D.; McKenna, G. B. *J. Non-Cryst. Solids* **1994**, *172–174*, 615–621.

3 Lacks, D.; Osborne, M. *Phys. Rev. Lett.* **2004**, *93*, 255501.

4 O'Connell, P.; McKenna, G. B. *Mech. Time-Dependent Mater.* **2002**, *6*, 207–229.

5 Bernstein, B. *J. Rheol.* **1980**, *24*, 189–211.

6 McKenna, G. B. *J. Phys.-Condens. Matter* **2003**, *15*, S737–S763.

7 Struik, L. *Polymer* **1997**, *38*, 4053–4057.

8 Waldron, W.; McKenna, G. B. *J. Rheol.* **1995**, *39*, 471–497.

9 Hasan, O. A.; Boyce, M. C. *Polymer* **1993**, *34*, 5085–5092.

10 Casas, F.; Alba-Simionesco, C.; Lequeux, F.; Montes, H. *J. Non-Cryst. Solids* **2006**, *352*, 5076–5080.

11 Hoy, R.; Robbins, M. *J. Chem. Phys.* **2009**, *131*, 244901.

12 Hoy, R.; Robbins, M. *Phys. Rev. E* **2008**, *77*, 031801.

13 Lyulin, A. V.; Michels, M. A. *J. Phys. Rev. Lett.* **2007**, *99*, 085504.

14 Boyce, M.; Arruda, E. *Polym. Eng. Sci.* **1990**, *30*, 1288–1298.

15 G'Sell, C.; Souahi, A. *J. Eng. Mater. Technol.* **1997**, *119*, 223–227.

16 Meijer, H.; Govaert, L.; Smit, R. Toughening of Plastics: Advances in Modeling and Experiments; American Chemical Society: Washington D.C., **2000**; pp 50–70.

17 Buckley, C.; Dooling, P.; Harding, J.; Ruiz, C. *J. Mech. Phys. Solids* **2004**, *52*, 2355–2377.

18 Hasan, O. A.; Boyce, M. C.; Li, X. S.; Berko, S. *J. Polym. Sci. Part B: Polym. Phys.* **1993**, *31*, 185–197.

19 McKenna, G. B.; Zapas, L. *Polym. Eng. Sci.* **1986**, *26*, 725–729.

20 Van Melik, H.; Govaert, L.; Raas, B.; Nauta, W.; Meijer, H. *Polymer* **2003**, *44*, 1171–1179.

21 Yee, A.; Bankert, J.; Ngai, K.; Rendell, R. *J. Polym. Sci. Part B: Polym. Phys.* **1988**, *26*, 2463–2483.

22 Yoshioka, S.; Usada, H.; Nanzai, Y. *J. Non-Cryst. Solids* **1994**, *172–174*, 765–770.

23 Lee, H.-N.; P. K.; Swallen, S.; Ediger, M. *Science* **2009**, *323*, 231–234.

24 Lee, H.-N.; Paeng, K.; Swallen, S.; Ediger, M. D. *J. Chem. Phys.* **2008**, *128*, 134902.

25 Lee, H.; Riggleman, R.; dePablo, J. J.; Ediger, M. D. *Macromolecules* **2009**, *42*, 4328–4336.

26 Rabinowitz, S.; Beardmore, P. *J. Mater. Sci.* **1974**, *9*, 81–99.

27 Liu, L.; Yee, A.; Gidley, D. *J. Polym. Sci. Part B: Polym. Phys.* **1992**, *30*, 221–230.

28 Liu, L.; Yee, A.; Lewis, J. *J. Non-Cryst. Solids* **1991**, *131–133*, 492–496.

29 Manson, J.; Hertzberg, R. Fatigue of Engineering Plastics; Academic Press: New York, **1980**.

30 Gacoin, E.; Chateauminois, A.; Fretigny, C. *Polymer* **2004**, *45*, 3789–3796.

31 Gacoin, E.; Fretigny, C.; Chateauminois, A.; Perriot, A.; Barthel, E. *Tribol. Lett.* **2006**, *21*, 245–252.

32 Chateauminois, A.; Fretigny, C.; Gacoin, E. Polymer Tribology; Imperial College Press: London, **2009**; Chapter 17, pp 559–581.

33 Rabinowitz, S.; Ward, I. M.; Parry, J. S. C. *J. Mater. Sci* **1970**, *5*, 29–39.

34 Bowden, F.; Tabor, D. The Friction and Lubrication of Solids; Oxford University Press: Oxford, **1964**.

35 Ferry, J. Viscoelastic Properties of Polymers, 3rd ed.; Wiley: New York, **1980**.

36 Masubuchi, Y.; Matsuoka, H.; Takimoto, J.; Koyama, K.; Ohta, Y. *Mater. Sci. Res. Int.* **1998**, *4*, 223–226.

37 Parry, E.; Tabor, D. *J. Mater. Sci.* **1974**, *9*, 289–292.

38 Weishaupt, K.; Krbecek, H.; Pietralla, M.; Hochheimer, H. D.; Mayr, P. *Polymer* **1995**, *36*, 3267–3271.

39 Allegra, G.; Raos, G.; Vacatello, M. *Prog. Polym. Sci.* **2008**, *33*, 683–731.

40 Berriot, J.; Lequeux, F.; Montes, H.; Pernot, H. *Polymer* **2002**, *43*, 6131–6138.

41 Montes, H.; Lequeux, F.; Berriot, J. *Macromolecules* **2003**, *36*, 8107–8118.

42 Bodiguel, H.; Lequeux, F.; Montes, H. *J. Stat. Mech.-Theory Exp.* **2008**, P01020.

43 Lyulin, A.; Hudzinskyy, D.; Janiaud, E.; Chateauminois, A. *J. Non-Cryst. Solids* **2011**, *357*, 567–574.

44 Mindlin, R. ASME Transactions, *J. Appl. Mech. Ser. E* **1953**, *16*, 327–344.